Verifying Machine Learning conclusions for securing Low Inertia systems

Bellizio, Federica; Bugaje, Al Amin B.; Cremer, Jochen L.; Strbac, Goran

DOI
10.1016/j.segan.2022.100656

Publication date
2022

Document Version
Final published version

Published in
Sustainable Energy, Grids and Networks

Sustainable Energy, Grids and Networks 30 (2022) 100656

Contents lists available at ScienceDirect

Sustainable Energy, Grids and Networks

journal homepage: www.elsevier.com/locate/segan

Verifying Machine Learning conclusions for securing Low Inertia systems

Federica Bellizio [a], Al-Amin B. Bugaje [a], Jochen L. Cremer [b,*], Goran Strbac [a]

[a] Imperial College London, South Kensington, London SW7 2BU, United Kingdom
[b] TU Delft, Mekelweg 5, 2628 CD Delft, The Netherlands

ARTICLE INFO

Article history:
Received 16 October 2021
Received in revised form 27 January 2022
Accepted 8 February 2022
Available online 22 February 2022

Keywords:
Low Inertia system
Machine Learning
Dynamic Security Assessment
Power systems operation
Probabilistic security

ABSTRACT

Machine Learning (ML) for real-time Dynamic Security Assessment (DSA) promises a probabilistic approach to secure lower safety margins and costs. However, future systems with a high share of renewables have low inertia and converter-interfaced devices resulting in faster dynamics. Past research on ML-based DSA used high inertia systems to study 'the best' ML data, features, and models building upon each other's work for decades. Seldom has ML-based research for DSA questioned whether the underlying assumptions for (and the conclusions of) these studies are still valid for low inertia systems.

This work studies exemplary changes in assumptions (and conclusions) for ML-based DSA when moving from High Inertia (HI) to Low Inertia (LI) systems. The dynamical system of the LI system is brought in perspective with the most typical ML-based approaches, which are organised in sequential steps. The steps consider the generation of the training database, the data pre-processing and feature selection, the model training and validation. This work analyses each step individually for the changed assumptions in the dynamical LI system, and subsequently, a case study provides the evidence that considering a LI system to identify the 'best' ML approaches is important. The case studies on IEEE 14 and 68 bus systems confirm that LI systems must be optimised for security (otherwise, they result in 80% less security than HI systems). The key findings, however, are that using ML makes significantly more sense in LI systems than in HI systems as the LI dynamics are in shorter timescales (and the advantage of ML is to predict security in milliseconds) and that secure/insecure operations can be separated more straightforwardly in LI systems as ML increases the accuracy by up-to 40% towards close to 100% when using neural networks.

1. Introduction

Power system operation with a high share of renewables becomes more uncertain and has lower inertia to respond securely to disrupting dynamics [1,2]. Not only new renewable generation but also new flexible loads and new transmission devices have completely different dynamics than conventional synchronous generations with which the power system was designed. These new technologies are interfaced with converters that result in lower inertia in the system [3] and faster dynamics, as the technology can interact and generate unexpected time couplings with existing system components as synchronous generators [4,5]. The timescale of such relevant dynamics is similar to electromagnetic transients (and gets reduced from a few microseconds to several milliseconds as shown in Fig. 1). In response, operators can harden the power infrastructure or develop new software tools for uncertain operation (much cheaper) to keep up the security of supply [2]. Unfortunately, most current real-time software tools are limited to only the assessment of the static security of a shortlist of system faults. With current software, the assessment of the dynamic security is infeasible in real-time as they require time-domain simulations that have long computational times as they rely on numerical integration [6,7] (e.g., 56 s for the French system [8]).

Methods from ML show high potential for real-time probabilistic DSA [9,10]. The idea is to carry out simulations offline, then train an ML model offline that can be used in real-time for predicting the security instead of simulating it. This approach is a promising idea as ML predictions require nearly zero computational time, and hence very large numbers of possible operating conditions (OCs) can be assessed in real-time for a very large number of possible fault scenarios. In the last decades, many researchers investigated this idea with different settings [11,12]. Most works, however, propose the same sequence of steps

* Corresponding author.
E-mail addresses: f.bellizio18@imperial.ac.uk (F. Bellizio), al-amin.bugaje18@imperial.ac.uk (A.-A.B. Bugaje), j.l.cremer@tudelft.nl (J.L. Cremer), g.strbac@imperial.ac.uk (G. Strbac).

https://doi.org/10.1016/j.segan.2022.100656

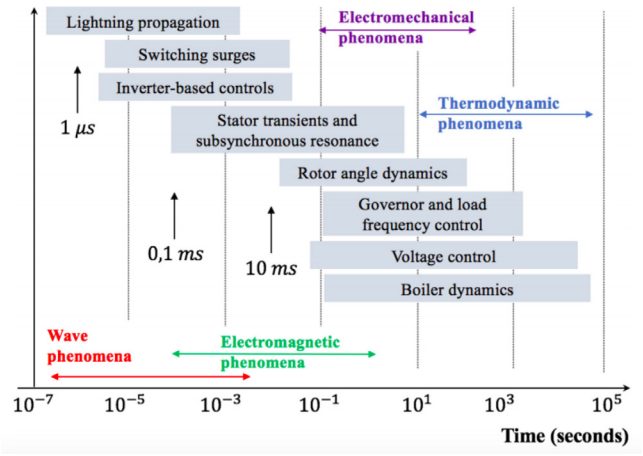

Fig. 1. Timescales in low inertia systems [5].

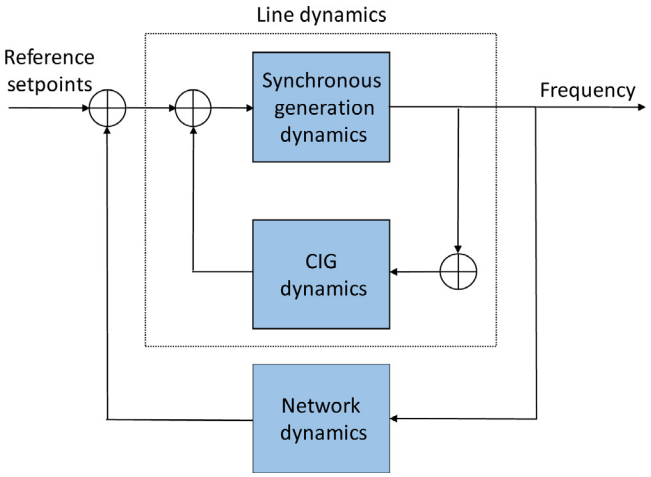

Fig. 2. Block diagram of LI network.
Source: modified version of [23]).

from generating data over data pre-processing, selecting features towards training and validating the ML model. These works analysed the individual steps in detail, e.g. for data generation [13, 14], for data processing and feature selection (FS) [15–17], for model training [18,19] and selection. Over decades this line of research has built upon each other improving successively previous conclusions in each of the steps. However, most of the works following this ML-based idea have carried out their studies on standard IEEE test systems, which typically assume HI in their dynamical models representing power systems from the past. Unfortunately, most works do not consider large amounts of renewable energy sources or adequate demand models and their flexibility or converter-interfaced generations or storage.

This paper aims to investigate whether the conclusions in ML-based real-time DSA made in the past HI systems are still valid for LI systems. A few research has considered more LI-based assumptions in their proposed ML-based DSA concepts. For instance, [20] considers 30 % renewable energy sources, HVDC links, and forecasts for 2030 for generating OCs, but the static and small-signal analysis does not involve simulating the full dynamic model. [21] considers dynamic models for converter-interfaced generators (CIGs) and assumes uncertainty in photovoltaic and wind power.

This paper has three contributions that offer insights, for the first time, on whether the conclusions from ML-based DSA on HI systems can be transferred to LI systems. These insights are important to verify which findings from past research in ML-based DSA need to be revisited and how researchers may carry out ML-based research for LI DSA in the future. The first contribution summarises the changing assumptions of dynamics LI power systems that influence ML-based DSA, including the dynamical modelling of CIGs, transmission lines, and loads. The second contribution is analysing the impact of these assumptions on ML-based DSA. The impact of each assumption is analysed for each step individually in the ML-based DSA. The third contribution proposes a modified test system in the case study that corresponds to a LI system and can be used for ML-based research for DSA. Case studies on the original and the proposed modified versions of the IEEE test systems with 14 and 68 buses compare the performance of ML-based DSA in HI and LI systems considering transient stability. The rest of the paper is structured as follows. Section 2 describes the full dynamical model of the future low inertia system. Section 3 discusses the impact of the new dynamics on the ML-based security rules. Subsequently, Section 4 presents the case study, and Section 5 concludes the paper.

2. Dynamic security of low-inertia systems

This section describes the general ordinary differential equation (ODE) formulation of the dynamical model of LI systems [22]. In addition, this section introduces the new security definition and the new classes of security for such systems.

The nodal and generation sets are N and G, respectively, where G includes synchronous generators S and converter-interfaced generators C, i.e. $G = S \cup C$. The set C is further classified into grid-forming converters $C_F \subset C$ and grid-following $C_f \subset C$ converters. The dynamical model of LI system (Fig. 2) can be then described as follows:

$$\dot{x} = f(x, u) \tag{1}$$

where

$$\begin{aligned} x =& (x^F_{c_1}, \ldots, x^F_{c_{c_F}}, x^f_{c_1}, \ldots, x^f_{c_{c_f}}, x_{g_1}, \ldots, x_{g_S}, x_n) \\ u =& (u^F_{c_1}, \ldots, u^F_{c_{c_F}}, u^f_{c_1}, \ldots, u^f_{c_{c_f}}, u_{g_1}, \ldots, u_{g_S}) \end{aligned} \tag{2}$$

are the system states and inputs, respectively. The models of the dynamical components to consider in LI systems, i.e. CIGs, synchronous generators, loads and transmission lines, are described in the following sections.

2.1. Dynamics of converter-interfaced generators

A three-phase power converter model is considered for both grid-forming and grid-following operation mode. The two operation modes are shown in Fig. 3. The model consists of a DC-link capacitor, a lossless switching block, which transforms the DC voltage v_{dc} into a three-phase AC voltage v_{sw}, and an output RLC filter (r_f, l_f, c_f). The detailed description of the dynamical model of CIGs, including a filter, transformer, AC-side controller and Phase-Locked Loop (PLL), can be found in [22].

Given these dynamics, the following state and control inputs can be defined for CIGs:

$$\begin{aligned} x^F_c =& (i_f, v_f, i_g, \xi, \tilde{p_c}, \tilde{q_c}, \theta_c) \\ x^f_c =& (i_f, v_f, i_g, \xi, \varepsilon, \theta_s, \tilde{p_c}, \tilde{q_c}, \theta_c) \\ u^F_c =& (p^*_c, q^*_c, V^*_c, \omega^*_c, v^*_{dc}) \\ u^f_c =& (p^*_c, q^*_c, v^*_{dc}) \end{aligned} \tag{3}$$

with v_f and i_f the filter voltage and current, i_g the transformer current that is injected into the grid and $(\tilde{p_c}, \tilde{q_c})$ the internal state

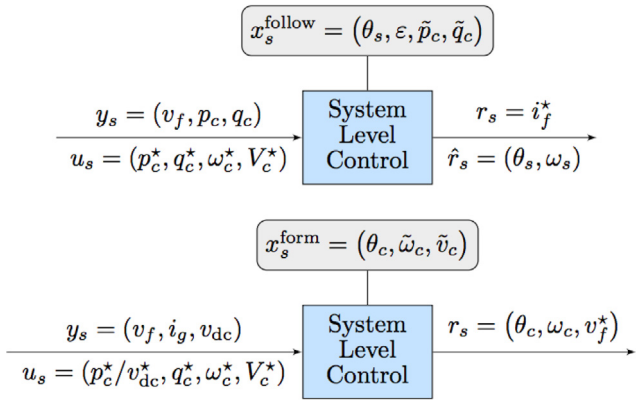

Fig. 3. System-level control of grid-following operation mode (top) and grid-forming operation mode (bottom) [22].

variables. ε and ξ are the integrator states, θ_c is the reference angle at which the AC-side controller operates and θ_s is the estimate of the phase angle from the PLL. Finally, ω_c^*, V_c^*, p_c^*, q_c^* represent the setpoints for frequency, voltage, active and reactive power, respectively.

2.2. Dynamics of synchronous generators

For a traditional two-pole synchronous generator, the internal dynamics are described by the swing equation:

$$M_g \dot{\omega}_r = \Delta p_e - D_g(\omega_r - \omega_0) \tag{4}$$

with M_g and D_g the inertia and damping constants and Δp_e the difference between mechanical and electrical power at the generator's output.

2.3. Load dynamics

Dynamic models of loads express the active and reactive powers as a function of voltage and time. Two main dynamical models for loads can be distinguished, the inductive model, and the exponential recovery load model [24]. These two models are mainly characterised by different time recovery ranges following disturbances. The inductive model is derived from the equivalent circuit of an induction motor with static and rotor resistances corresponding to a recovery time in the range of seconds (similar to electromagnetic transients). In this model, the active and reactive power, and hence the load current, are represented as functions of the past and present voltage magnitude and frequency of the load bus allowing to inject or withdraw current from the bus instantaneously when needed (current injection model [25]). Conversely, the exponential recovery load model is used to represent loads that slowly recover from a disturbance over large time periods (from several seconds to tens of minutes, similar to electromechanical transients).

2.4. Transmission line dynamics

Grid dynamics are typically neglected in synchronous generator-dominated power systems as these dynamics are much faster than those of the excitation and governor systems. With the inclusion of fast-acting CIGs, the line dynamics become relevant as they are of the same order of magnitude as the ones of converters (electromagnetic phenomena). The line dynamics can be represented using a conventional RL formulation:

$$\dot{i}_{jk} = \frac{\omega_b}{l_{jk}}(v_{nj} - v_{nk}) - \left(\frac{r_{jk}}{l_{jk}}\omega_b + j\omega_b\omega_c^*\right) i_{lj}, \forall j \in N, k \in K_j \tag{5}$$

with i_k and v_n being the nodal current and voltage, r_{jk} and l_{jk} being the resistance and inductance of the line connecting $j \in N$ and $k \in K_j$ where $K_j \subset N$ is the subset of nodes adjacent to node j.

2.5. Security definition and classification

There is a need for new considerations on the classification and definition of the power system stability phenomena as a result of the increasing share of CIGs into bulk power systems [5]. The different dynamic behaviour of CIGs compared to synchronous generators behaviour leads to a mix of new types of transient phenomena that need to be constantly assessed. As long as the dynamic response to a fault affects only the CIG and does not cause the cascading instability of the main system, the conventional definition of power system security still applies. The conventional definition of security defines the ability of an electric power system to withstand sudden disturbances without major service interruptions in real-time. However, two new stability classes, i.e. converter-driven stability and resonance stability, need to be considered as the integration of power electronics devices scales the timescale of interest down to electromagnetic transients (Fig. 1). Resonance instability occurs when the magnitudes of voltage, current or torque exceed specific thresholds following the oscillations of periodic energy exchanges. These instabilities are caused by the resonance between series compensation and the mechanical torsional frequencies of the turbine-generator shaft (i.e. torsional resonance) or by the resonance between the series compensation and the electric characteristics of the generator (i.e. electrical resonance). Converter-driven instabilities involve a wide range of unstable frequency oscillations due to cross-couplings of CIG control loops with both the electromechanical dynamics of machines and the electromagnetic transients of the network.

The integration of CIGs does not affect the stability definitions for the existing stability classes, i.e. rotor angle, voltage and frequency stability. In terms of rotor angle stability, there is no consensus regarding the effects of CIGs on the small disturbance rotor angle stability. However, the fast control of such converters during and after the fault can significantly influence the transient rotor stability. Regarding voltage stability, the new dynamics of fast-acting load components, e.g. induction motors, controlled loads, HVDC links, may represent new potential causes of instabilities. Finally, although CIGs do not provide an inertial response as they are typically associated with renewable sources, they can provide fast primary frequency response, and this is crucial in LI systems in which fast controllers are needed to arrest frequency drops and keep the system's frequency within the acceptable range at all times.

3. ML-based security rules for LI systems

This section investigates the impact of increasing the share of CIGs on conventional ML-based approaches for DSA. The four steps of these approaches are shown in Fig. 4, i.e. data generation, data pre-processing, model learning and model validation [11]. The following investigates these steps one by one with regards to past HI-based assumptions that may be outdated in LI systems.

3.1. Data generation

In conventional data-driven DSA workflows, database generation is the pivotal first step that lays a foundation for training a good quality model, and it is usually performed offline, starting from a list of possible OCs. The final database is a collection of these OCs that serve as pre-fault states, together with their

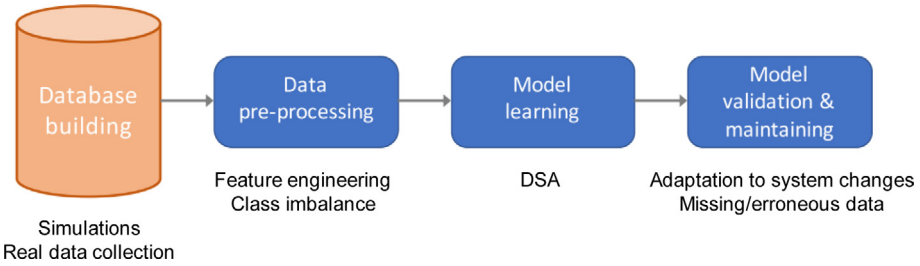

Fig. 4. ML-based workflow for DSA [11].

respective post-fault security status after a contingency. In generating the pre-fault states, a combination of possible load levels and generator parameters are matched by solving the optimal power flow. In situations where historical data is insufficient, the loads are sampled from a multivariate normal distribution that assumes some correlation between the loads [13,14]. In the future, power systems with high renewable sources integration challenge this status quo with increased uncertainty. Firstly, there is a need to consider more "rare" cases that were previously ignored. Secondly, the search space that defines the OCs becomes much larger than that of current power systems. Current OCs of a power system are defined by a predefined set of variables, also known as features, i.e. currents, active and reactive power injections, load levels, bus voltages and phase angles. However, in future LI systems, the number of features to consider for each OC is expected to be significantly larger as each CIG will be, in turn, characterised by the terminal current/voltage. Therefore, generating possible OCs becomes more computationally intensive [20].

3.2. Data pre-processing

Once the data is generated, the data is typically processed before being fed to a learning algorithm. This step becomes necessary in future LI systems to improve the predictive performance, reduce the training time and make the training data more interpretable. Many features are necessary to describe the OC of LI systems, and thus, the input features are expected to be highly redundant. Redundancy is one of the leading causes of low predictive performances in ML classifiers. Consequently, considering a large set of input features significantly increases the training time, making the training computationally infeasible in large systems even if done offline. FS supports reducing the training time and improves the quality of predictions by selecting the features most relevant to the given classification target, and hence reducing the input space [20]. However, some of the most accurate FS approaches, i.e. wrapper methods and embedded methods, are very time-consuming. Therefore, their performance on the large input spaces of future OCs should be further investigated. Conversely, filter methods are another class of FS approaches based on statistical tests, which are fast even on large input spaces but generally result in low predictive performance [26].

3.3. Model learning

The high complexity of the dynamics of LI systems could be one of the leading causes of the low predictive performance of ML-based models for DSA. The dynamics of synchronous generators, CIGs and transmission lines have significant differences in the time constants. Training a single classifier for such different timescales could result in very low accuracies. A classifier that works for short timescales, such as converters, may not work on much longer timescales such as turbines. Therefore, different models for each generator/converter insecurity pattern may be required to improve the predictive performance in a real-time setting. Clustering the different dynamics following the clearing of a fault and then training a different classifier for each cluster of dynamics could be a potential solution to overcome this challenge [21]. Since DTs have been proven to be suitable for real-time DSA purposes, multiple DTs may be used for these clusters of dynamics.

3.4. Model validation and real-time assessment

The increasing uncertainty in future power system operations resulting from the integration of renewable sources will significantly impact the quality of prediction of the ML-based models for DSA. In the traditional two-stages workflow of these approaches, the time distance between the offline and real-time stages compromises the performance of the offline trained classifier as the real-time OCs may be very different from those included in the training database. In such an uncertain scenario, training the classifier on immediate-future states or periodically updating the classifier may overcome the challenge of frequent changes in the distributions of the OCS [18,19,21]. However, these updates are computationally challenging as they are carried out in the real-time environment to minimise as much as possible the discrepancies between offline and real-time OCs. Therefore, the retraining or updating of the model with new data acquisition needs to be very fast [17].

4. Case study

This section studies the impact of lowering the inertia on ML-based DSA. ML-based workflows for DSA were designed in HI systems and may not be valid anymore in LI systems. This case study aims at demonstrating this impact on each step individually in the ML-workflow (i.e. data generation, data pre-processing, and model learning/validation). Subsequently, this study analyses the individual findings to provide insights on whether past research in ML-based DSA needs to be revisited or can be assumed as granted for LI systems and if the findings and assumptions also transfer to larger systems, such as to the IEEE 68-bus system.

The tested HI and LI systems had different assumptions. The tested HI systems were the original IEEE 14-bus [27] and IEEE 68-bus systems [28]. In these two HI systems, the dynamics were governed exclusively by synchronous generation and only static transmission lines. The tested LI systems were modifications of the IEEE 14 and 68-bus systems, where all the static transmission lines were replaced by dynamic lines, except the faulted line, and the 40 % and 25 % of thermal generation was replaced by CIGs in the IEEE-14 bus and IEEE-68 bus systems, respectively. The considered CIGs (the model in Section 2.1) were wind farms of similar power rating to the replaced synchronous generators. The wind farm model is a static generator connected to the network through the inverter model shown in Fig. 5 [29,30]. The control of power systems assumed an inner current control loop and an outer voltage control loop. The two systems were modelled in

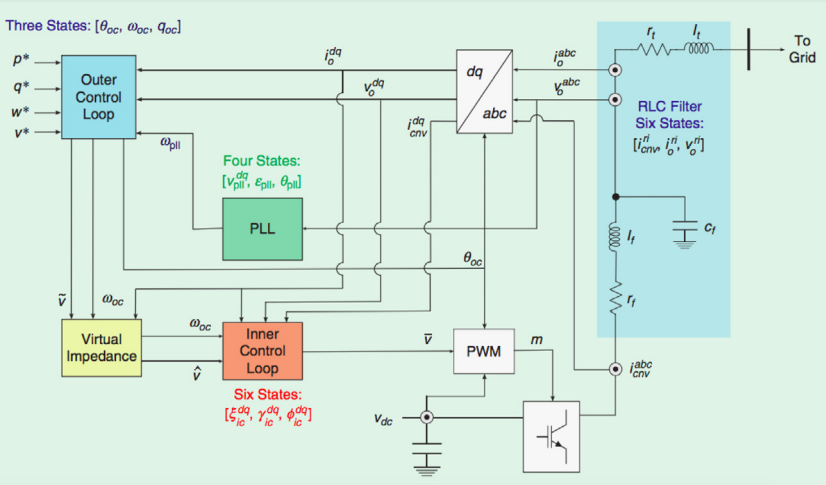

Fig. 5. The block diagram of the grid-supporting inverter of wind farm models [29].

Julia 1.6.2 with the packages *PowerSystems.jl* [30], *PowerSimulationsDynamics.jl* [29]. Most of the defaults settings of the inverters for the LI system were used. The damping constant and the frequency droop gain of the outer controller were reduced by 99% to assume faster controls in the future and to study the impact of the faster controls with lower inertia on future system security.

The training data included $|\Omega| = 10{,}000$ pre-fault OCs and corresponding post-fault security labels for each of the HI and LI test systems. The pre-fault OCs considered different sampled setpoints for active and reactive power injections. The active load setpoints were sampled from a multivariate Gaussian distribution with a Pearson's' correlation coefficient $c = 0.75$. The method of inverse transformation was used to convert to a marginal Kumaraswamy distribution, where $a = 1.6$, $b = 2.8$ are distribution shape parameters. Then, the active load setpoints were scaled to be within $\pm 25\%$ and $\pm 10\%$ of the nominal values for the 14 and 68 bus system, respectively. The reactive powers followed the active powers proportionally as constant impedances were assumed. The AC power flow was then computed with the Newton–Raphson algorithm to obtain pre-fault OCs power generation. The solution to the AC power flow provides the full pre-fault variables X_i for each OC $i \in \Omega$, where the variables are active and reactive power generations, active and reactive power loads and voltages magnitudes and phase angles. The post-fault security label considered the transient security for 3 different three-phase faults k on line 2–3 (Fault 1), 3–4 (Fault 2), and 2–5 (Fault 3) for the 14 bus system (Fig. 6) and for a fault on line 31–38 for the 68 bus system (Fig. 7) with each a clearance time of 0.6 s. The fault on line 2–3 for the 14 bus system was used for the following studies unless indicated otherwise. If within 10 s simulation time after the fault, all differences between each two phase angles of the generators were less than 180°, than the OC i was considered transient secure $Y_{i,k} = 1$, otherwise insecure $Y_{i,k} = 0$ and with that, the security label was computed. These transient simulations were modelled with the same packages *PowerSystems.jl* and *PowerSimulationsDynamics.jl*. The simulations were solved with the IDA package from Sundials solvers [31]. These simulations were performed twice, evaluating the security labels for the two systems, the HI and LI systems. The pre-fault OC and post-fault labels built the different databases for evaluating the impact on the ML workflow for DSA. All simulations were carried on a standard machine with six cores and 16 GB RAM.

The ML-methods studied included different FS methods as Minimum Redundancy Maximum Relevance (MRMR), Correlation-based Feature Selection (CFS), Joint Mutual Information (JMI), Support Vector Machine Recursive Feature Elimination (SVM-RFE), Sequential Forward Selection (SFS) and different ML models, as Decision Trees (DTs), SVMs, XGBOOST, feed-forward Artificial Neural Networks (ANNs). A linear kernel for the SVM, 50 estimators for the XGBoost and 3 layers with 30, 15 and 5 neurons for the ANN, were used. Across the studies, 5 different combinations of training/testing sets were computed for each classification model. DTs were used to measure the classification performance unless indicated otherwise. The F1-score was most of the time used to assess classification performance as this score penalises the false negative and false positive. The false negatives have the highest cost in power system DSA (as false negatives can result in partial power blackouts in the worst case). For the fault on line 2–3, 9000 OCs were used for training with a split of 70%/30% for training/testing and the remaining 1000 OCs for validation. For the other faults, 600 OCs were used for training with a split of 70%/30% for training/testing and the remaining 100 OCs for validation.

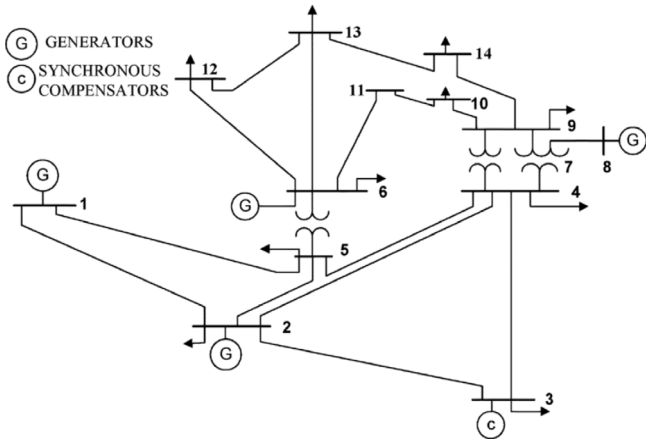

Fig. 6. The IEEE 14-bus system with three-phase faults on lines 2–3, 2–5 and 3–4.

4.1. Differences in generating data for HI and for LI systems

This study focuses on the differences between an HI and an LI system when generating ML training data. The study focuses on three parts as a good training database for ML-based DSA (i) avoids redundancy in the data e.g., balanced shares of secure/insecure data, (ii) is easily separable (e.g., by a binary

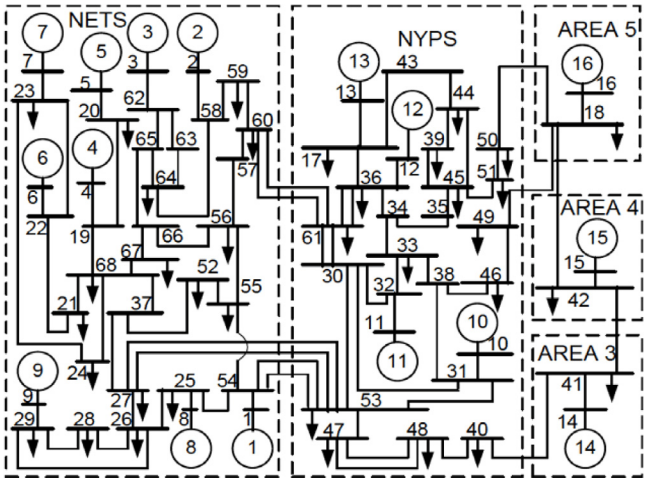

Fig. 7. The IEEE 68-bus system with three-phase fault on line 31–38.

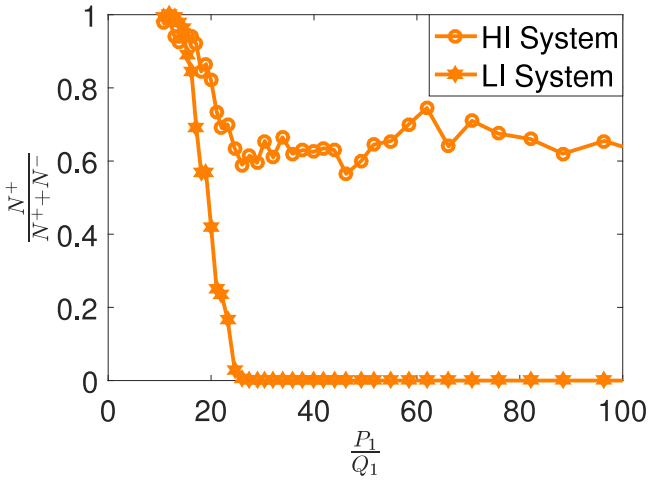

Fig. 8. Share of secure OCs with increasing load levels for HI and LI systems.

classifier), and (iii) is small while containing high levels of information.

The analysis (i) investigated the redundancy in the database. The share of secure/insecure OCs was a metric to investigate this redundancy, e.g., if all OCs in the database are secure, an ML model cannot learn a security rule for classifications. Fig. 8 shows the share of secure OCs $\frac{N^+}{N^+ + N^-}$ in the HI and LI system for the same feature $\frac{P_1}{Q_1}$ active/reactive power generator level. Each point in the figure represents an average of secure OCs over 200 OCs with similar $\frac{P_i}{Q_i}$ values. The share of secure OCs decreased with increasing power generation in the two systems. However, the decrease in the LI system was much steeper and quickly converges to almost no secure OCs. This analysis showed that LI systems must be improved to keep the security as high as in HI systems (the tested LI system was not optimised for security), and the steep decrease showed the importance of optimising power generations to ensure the system's security.

The analysis (ii) investigated the separability of the data. Fig. 9 shows the distributions of secure and insecure OCs for the two systems, HI and LI, according to two generator power levels (active and reactive). A key finding was that the data is more separable in the LI system than in the HI system, e.g., even a linear function could separate secure from insecure OCs in the LI system, however, the security boundary (that is the function separating the secure from insecure OCs) seemed highly non-linear in the HI system (at least in these two features). The high non-linearity of the input data in the HI system suggested that in such a system (i) more training features than in the LI system would be needed to obtain similar accuracy performance, (ii) the dependence between system security and changes in power generations is not as strong as in LI systems. In LI systems, small changes in the generation make the system highly secure/insecure and this dependence results in a clearly defined boundary. Fig. 9 is zoomed in to better show the separating boundary between the secure/insecure OCs. When zooming out, some rare OCs (clearly separated from the others) can be noticed in both systems. Their number was reduced by 40% in the LI system compared to the HI system.

The analysis (iii) investigated the information per data (efficiency of database) in two methods: the first method was to train classifiers for the two systems with varying training database sizes, figuring out the classifiers with the same predictive performance, and the second method was to analyse the information content of the two databases for LI and HI systems. In the first method, DTs were trained for the two systems for different sizes of training database Ω then their F1-score performances were analysed. Fig. 10 shows that the F1-score performance increased in the two systems. However, the F1-score was significantly higher in the LI system, which is related to the easier separability as pointed out in analysis (ii) and Fig. 9. The low DT performance in the HI system is related to the small test system size as in small systems, faults may result in very complex transients, which may be difficult to predict. These low numbers of around $\sim$ 80% were also found for the IEEE-68 bus system Section 4.4, and in the literature, e.g., [17]. Additionally, the LI system classifier was very robust against reductions of the training database varying only around 2% compared to 20% in the HI system. In the second method, the mutual information I was computed to study the information content of the two training databases with the same size for HI and LI systems. The mutual information I between feature subsets and target Y and a summary of the two analyses, (i–ii) are in Table 1. The higher information in features X_i about the target Y resulted in higher classification performance in the LI system. The accuracy and F1-score were higher in LI than in HI systems, respectively by 23%, and 39%. The findings of high classification performance, the improved separability of security/insecurity in LI systems, seem promising for a key role of ML for future real-time DSA.

4.2. Selecting features in LI systems

This study focuses on the differences between a HI and a LI system when pre-processing data to select features, the second step in ML-based workflows for DSA. Effective pre-processing of data reduces redundancy, enhances classification performance and reduces the training computational times. The past research on HI systems showed two findings: (i) the active and reactive power levels of generators are effective features for DSA, and (ii) typically, the wrapper and embedded FS methods have the highest performance for offline applications, and the filter FS methods are the fastest and hence best for real-time applications. The following two analyses investigate whether the same findings hold for LI systems.

The analysis (i) investigates the importance of the feature subsets power generations, power loads, voltage magnitudes and phase angles. This analysis used two metrics, the F1-score of a trained DT and the mutual information $I(X;Y)$. The analysis restricts the training data X to the corresponding feature subset. In other words, the subset providing the highest F1-score and

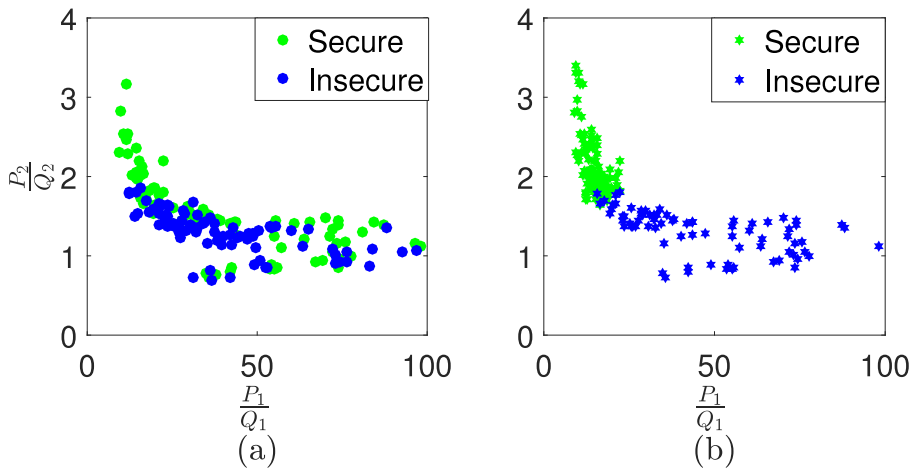

Fig. 9. Secure and insecure OCs are less separable in (a) HI systems than in (b) LI systems.

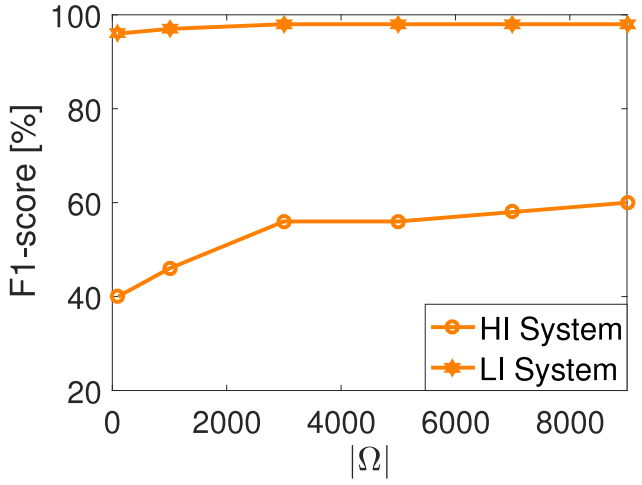

Fig. 10. Prediction performance for different training database sizes.

Table 1
Performance metrics of training database.

	$\frac{N^+}{N^+ + N^-}$	$I(X;Y)$	Accuracy	F1-score
HI system	0.7	2.1	75.3%	59.2%
LI system	0.2	10.4	97.8%	98.5%

mutual information are the best features. This analysis was undertaken for the LI and HI systems, and the results in Table 2 show that the subset of power generations was the best feature subset in both systems. E.g., in the HI system, the F1-score is 20 % higher when choosing power generation as features than when choosing other features. This finding is aligned with Fig. 9 which showed power generation as a strong indicator for system security in LI systems. However, in LI systems, voltage phase angles show to provide significantly higher mutual information, and this is also confirmed in the literature, as voltage phase angles have conditional correlation properties allowing to capture the system's topology, and hence more relevant information for the security [32].

The analysis (ii) investigates whether the same FS methods are the best in LI systems as in HI systems, where the different FS methods select the best features out of all available features. For each different FS method, a DT was trained on the selected features. Then, the DT classification performance was compared to identify the best FS method for the LI system and for the HI system. The compared FS methods were MRMR, CFS JMI as filter method, SVM-RFE as embedded methods, and SFS as wrapper methods. The results in Table 3 show that the embedded method SVM-RFE and the wrapper method SFS had the highest F1-scores in the LI and HI systems, respectively. The analysis showed that SFS selected power generation and voltage phase angles feature as the mutual information values and F1-scores were high (Table 2). Similarly, SVM-RFE selected most features from voltage phase angles according to the high mutual information value as in Table 2. However, SVM-RFE also selected features from power generation and loads as they improved the accuracy.

These two analyses showed that the conclusions made in the past that corresponded to data pre-processing in ML-based workflows remain valid in the future LI systems: wrapper and embedded approaches typically result in the highest classification performance.

4.3. Training ML models for LI and HI systems

This study aims at investigating whether the classification models recommended for HI systems will still be high-performing in future LI systems. The best ML model and the criteria to select the best model highly depend on the type of problem and application. In the following criteria finding a good trade-off between interpretability of the model and accuracy (F1-score) of the model was studied as an example [33]. The models studied were DTs, SVM, XGBoost, and feed-forward ANN and the training considered all the 60 available input features. Cross-validation was used to tune the hyper-parameters of the models.

The results in Table 4 show that ANN outperforms the other models in LI and HI systems in terms of the F1-score. E.g., ANN outperforms SVM by around 8 % and 2 %, in HI and LI systems, respectively. The performance however of all models improved from HI to LI systems which were caused by the higher separability in LI systems as discussed earlier with Fig. 9. However, the values in the HI system are generally lower than what has been reported in the literature which is caused by the hard DSA classification problem at hand. The system security is represented by a highly non-linear security boundary and it seemed challenging to predicting for these selected faults with little training data and high load variability. Interestingly, the DTs showed high F1-score accuracy in LI systems of up to 98.5%. Additionally, DTs were promising regarding the selecting criteria of the trade-off to interpretability, as DTs offer higher levels of interpretability over ANN models. Other criteria can be selected in different applications, e.g. accuracy performance is prioritised in energy and load forecasting applications where ANN can be preferable [34,35].

Table 2
F1-score (of trained DTs) and mutual information I for different feature subsets.

		Power generation	Power loads	Voltage angles	Voltage magnitudes
HI system	F1-score	64.9%	46.3%	43.2%	42.6%
	$I(X;Y)$	0.5	0.5	0.6	0.5
LI system	F1-score	98.5%	97.2%	93.4%	95.8%
	$I(X;Y)$	1.7	2.4	4.7	1.6

Table 3
F1-scores of different FS methods for training DTs.

	CFS	MRMR	JMI	SVM-RFE	SFS
HI system	52.1%	60.4%	60.5%	62.0%	64.5%
LI system	98.2%	98.2%	98.5%	98.8%	98.7%

Table 4
F1-score with different classification models.

	DT	SVM	Xgboost	ANN
HI system	59.2%	55.4%	62.9%	63.1%
LI system	98.5%	97.2%	98.5%	99.1%

Table 5
Performance metrics for different faults.

		$\frac{N^+}{N^+ + N^-}$	$I(X;Y)$	Accuracy	F1-score
HI system	Fault 2	0.7	2.1	70.2%	47.5%
	Fault 3	0.7	2.1	72.5%	49.5%
LI system	Fault 2	0.6	11.9	93%	94.1%
	Fault 3	0.5	14.3	92%	94.2%

4.4. Larger LI systems and other faults

This study aims to generalise the previous studies to other faults (analysis i) and larger HI and LI systems (analysis ii). Analysis (i) investigated the 14-bus system with faults on two additional lines 3–4 (Fault 2) and 2–5 (Fault 3), and analysis (ii) investigated a fault on the IEEE 68-bus system.

The analysis (i) investigated whether the same conclusions for data generation, feature selection and model training (Sections 4.1–4.3) were drawn for other faults in the 14-bus system. The results in Table 5 show that the same conclusions can indeed be found for these faults. The LI system experienced more insecure OCs than the HI system as a result of the reduced inertia. The training features X_i had an information content about the target Y 10 times higher in the LI system resulting in an enhanced predictive performance with improvements of $\sim$ 20% in the accuracy and $\sim$ 45% in the F1-score. Again, the higher accuracy performance in the LI System resulted from the linear separating boundaries making the classification task much easier in the LI system than in the HI system.

The analysis (ii) investigated whether the same conclusions for data generation, feature selection and model training count also for a larger system, e.g. the IEEE 68-bus system. The results in Table 6 show that, indeed, most of the conclusions are the same. The share of secure OCs decreased by around 80% from the HI to the LI system. One difference is that the information content of the database was similar in the LI 68-bus system and the HI 68-bus system, and also the DT accuracy was similar. However, the F1-score performance was around $\sim$ 20% higher in HI than in LI systems.

These two analyses showed that most conclusions drawn in Section 4 for the overall workflow (Sections 4.1–4.3) generalise to different faults and on a large system.

Table 6
Performance metrics for a larger system.

	$\frac{N^+}{N^+ + N^-}$	$I(X;Y)$	Accuracy	F1-score
HI system	0.9	8.2	91.5%	77.1%
LI system	0.1	8.5	89.6%	94.5%

4.5. Discussion

The key finding of this work is that using ML for real-time DSA becomes even more promising in LI systems as it was already in HI systems. It is known that LI systems result in lower system security (when not optimised), but this paper's key insight is that the prediction of security (and learning of it by ML) becomes easier in LI systems. Additional findings of this work are the following differences (and similarities) when learning an ML model for a HI and a LI system:

1. When generating data, more OCs in LI systems may be insecure as the inertia is lower and dynamic couplings may occur.
2. The wrapper and embedded FS methods perform well in both LI and HI systems. Power levels are valuable features to assess future system security as lowered inertia results in a stronger dependence of system security to changes in power generations.
3. ML can easier learn the classification boundary in LI systems than in HI systems which results in strong improvements of security predictions. The reason for this improvement is that LI systems may have clear (e.g. linear) separating boundaries between secure/insecure OCs.
4. Wrapper methods for FS (such as SFS) result in the highest predictive performance, above all in HI systems. Therefore, they can be preferred when there are no limitations on computational resources, for example in the offline stage. Otherwise, a filter method such as JMI may be preferred.
5. ANNs result in the highest predictive performance in both LI and HI systems. However, DTs have a higher performance in LI than in HI systems, and hence are promising as DTs are more interpretable than ANNs.

This paper and its case study were designed for a typical ML-based workflow for DSA that corresponds to the majority of ML for DSA approaches from the literature. However, there may be other ML-based DSA approaches that use completely different workflows. For these workflows, the conclusions of this work are likely to correspond to as well as they relate to the underlying changes of the stability phenomena and how this changes the training data, however, this cannot directly be concluded from this work.

A limitation of this work is that the model and design of the LI system were not optimised. In contrast to some commercial software packages such as DSA Tools or PSS/E, the CIG model used in this work cannot differentiate between the types of generation behind or consider the weather conditions [36]. Advanced frequency modes and whether these influence the dynamics were not studied, and this paper is limited to the dynamic model used.

The analysis of advanced dynamic models and their impact on the overall system is an interesting analysis to conduct in the context of ML-based DSA aiming at predicting system security. This work, however, provided only the first step towards more sophisticated studies on ML-based real-time DSA for lower inertia power systems.

5. Conclusion

This paper aims at investigating whether findings from past research on Machine Learning approaches for DSA are still valid when moving from high to low inertia systems. ML is promising for real-time DSA as it can predict instantaneously the security, which becomes even more important in low inertia systems with shorter dynamic timescales. This paper describes the full dynamical model of future low inertia systems, including the dynamics of CIGs, loads, lines and synchronous generators. Then, this paper investigates the effect of these new dynamics on the design of ML-based approaches for real-time DSA. This design was successively optimised over the last decades but unfortunately only studied on high inertia systems. The studies on LI and HI IEEE 14 and 68-bus systems demonstrated the increased promising role of ML approaches in future ML-based DSA for LI systems. The predictive accuracies of these approaches improved by up to 40% and 20% for the 14 and 68 systems, respectively. ANNs and DTs show accuracies close to $\sim$ 99%. In the future, LI systems must be optimised for higher security, and regular updating of test systems is needed to develop future real-time DSA methods and tools.

CRediT authorship contribution statement

Federica Bellizio: Conceptualization, Data curation, Formal analysis, Investigation, Methodology, Validation, Writing – original draft. **Al-Amin B. Bugaje:** Data curation, Formal analysis, Validation, Writing – review & editing. **Jochen L. Cremer:** Formal analysis, Resources, Supervision, Visualization, Writing – original draft. **Goran Strbac:** Funding acquisition, Project administration, Supervision, Writing – review & editing.

Declaration of competing interest

The authors declare that they have no known competing financial interests or personal relationships that could have appeared to influence the work reported in this paper.

Acknowledgements

This work was supported by a scholarship funded by the Nigerian National Petroleum Corporation, NNPC, the TU Delft AI Labs Programme, NL, The Netherlands, and the research project IDLES, UK (EP/R045518/1).

References

[1] P. Panciatici, G. Bareux, L. Wehenkel, Operating in the fog: Security management under uncertainty, IEEE Power Energy Mag. 10 (5) (2012) 40–49, http://dx.doi.org/10.1109/MPE.2012.2205318.

[2] B. Kroposki, B. Johnson, Y. Zhang, V. Gevorgian, P. Denholm, B.-M. Hodge, B. Hannegan, Achieving a 100% renewable grid: Operating electric power systems with extremely high levels of variable renewable energy, IEEE Power Energy Mag. 15 (2) (2017) 61–73.

[3] J. Fang, H. Li, Y. Tang, F. Blaabjerg, On the inertia of future more-electronics power systems, IEEE J. Emerg. Sel. Top. Power Electron. 7 (4) (2018) 2130–2146.

[4] F. Milano, F. Dörfler, G. Hug, D.J. Hill, G. Verbič, Foundations and challenges of low-inertia systems, in: 2018 Power Systems Computation Conference, PSCC, IEEE, 2018, pp. 1–25.

[5] N. Hatziargyriou, J. Milanovic, C. Rahmann, V. Ajjarapu, C. Canizares, I. Erlich, D. Hill, I. Hiskens, I. Kamwa, B. Pal, P. Pourbeik, J. Sanchez-Gasca, A. Stankovic, T. Van Cutsem, V. Vittal, C. Vournas, Definition and classification of power system stability – revisited amp; extended, IEEE Trans. Power Syst. 36 (4) (2021) 3271–3281, http://dx.doi.org/10.1109/TPWRS.2020.3041774.

[6] P. Kundur, et al., Definition and classification of power system stability IEEE/CIGRE joint task force on stability terms and definitions, IEEE Trans. Power Syst. 19 (3) (2004) 1387–1401.

[7] L. Vanfretti, F.R.S. Sevilla, A three-layer severity index for power system voltage stability assessment using time-series from dynamic simulations, in: IEEE PES Innovative Smart Grid Technologies, Europe, IEEE, 2014, pp. 1–5.

[8] I. Konstantelos, G. Jamgotchian, S.H. Tindemans, P. Duchesne, S. Cole, C. Merckx, G. Strbac, P. Panciatici, Implementation of a massively parallel dynamic security assessment platform for large-scale grids, IEEE Trans. Smart Grid 8 (3) (2017) 1417–1426, http://dx.doi.org/10.1109/TSG.2016.2606888.

[9] T. Guo, J.V. Milanović, Probabilistic framework for assessing the accuracy of data mining tool for online prediction of transient stability, IEEE Trans. Power Syst. 29 (1) (2013) 377–385.

[10] J.L. Cremer, G. Strbac, A machine-learning based probabilistic perspective on dynamic security assessment, Int. J. Electr. Power Energy Syst. 128 (2021) 106571.

[11] L. Duchesne, E. Karangelos, L. Wehenkel, Recent developments in machine learning for energy systems reliability management, Proc. IEEE 108 (9) (2020) 1656–1676, http://dx.doi.org/10.1109/JPROC.2020.2988715.

[12] S. You, Y. Zhao, M. Mandich, Y. Cui, H. Li, H. Xiao, S. Fabus, Y. Su, Y. Liu, H. Yuan, H. Jiang, J. Tan, Y. Zhang, A review on artificial intelligence for grid stability assessment, in: 2020 IEEE International Conference on Communications, Control, and Computing Technologies for Smart Grids, SmartGridComm, 2020, pp. 1–6, http://dx.doi.org/10.1109/SmartGridComm47815.2020.9302990.

[13] V. Krishnan, J.D. McCalley, S. Henry, S. Issad, Efficient database generation for decision tree based power system security assessment, IEEE Trans. Power Syst. 26 (4) (2011) 2319–2327, http://dx.doi.org/10.1109/TPWRS.2011.2112784.

[14] F. Thams, A. Venzke, R. Eriksson, S. Chatzivasileiadis, Efficient database generation for data-driven security assessment of power systems, IEEE Trans. Power Syst. 35 (1) (2020) 30–41, http://dx.doi.org/10.1109/TPWRS.2018.2890769.

[15] F.R. Gomez, A.D. Rajapakse, U.D. Annakkage, I.T. Fernando, Support vector machine-based algorithm for post-fault transient stability status prediction using synchronized measurements, IEEE Trans. Power Syst. 26 (3) (2010) 1474–1483.

[16] H. Sawhney, B. Jeyasurya, A feed-forward artificial neural network with enhanced feature selection for power system transient stability assessment, Electr. Power Syst. Res. 76 (12) (2006) 1047–1054.

[17] F. Bellizio, J.L. Cremer, M. Sun, G. Strbac, A causality based feature selection approach for data-driven dynamic security assessment, Electr. Power Syst. Res. 201 (2021) 107537.

[18] M. He, J. Zhang, V. Vittal, Robust online dynamic security assessment using adaptive ensemble decision-tree learning, IEEE Trans. Power Syst. 28 (4) (2013) 4089–4098.

[19] T. Zhang, M. Sun, J.L. Cremer, N. Zhang, G. Strbac, C. Kang, A confidence-aware machine learning framework for dynamic security assessment, IEEE Trans. Power Syst. (2021) 1, http://dx.doi.org/10.1109/TPWRS.2021.3059197.

[20] R. Liu, G. Verbič, J. Ma, D.J. Hill, Fast stability scanning for future grid scenario analysis, IEEE Trans. Power Syst. 33 (1) (2018) 514–524, http://dx.doi.org/10.1109/TPWRS.2017.2694048.

[21] P.N. Papadopoulos, J.V. Milanović, Methodology for online identification of dynamic behavior of power systems with an increased amount of power electronics interface units, CSEE J. Power Energy Syst. 5 (2) (2019) 171–180, http://dx.doi.org/10.17775/CSEEJPES.2016.01180.

[22] U. Markovic, O. Stanojev, P. Aristidou, E. Vrettos, D.S. Callaway, G. Hug, Understanding small-signal stability of low-inertia systems, IEEE Trans. Power Syst. (2021) 1, http://dx.doi.org/10.1109/TPWRS.2021.3061434.

[23] Y. Jiang, R. Pates, E. Mallada, Dynamic droop control in low-inertia power systems, IEEE Trans. Automat. Control (2020).

[24] A. Arif, Z. Wang, J. Wang, B. Mather, H. Bashualdo, D. Zhao, Load modeling—A review, IEEE Trans. Smart Grid 9 (6) (2018) 5986–5999, http://dx.doi.org/10.1109/TSG.2017.2700436.

[25] B. Stott, Power system dynamic response calculations, Proc. IEEE 67 (2) (1979) 219–241, http://dx.doi.org/10.1109/PROC.1979.11233.

[26] I. Guyon, A. Elisseeff, An introduction to variable and feature selection, J. Mach. Learn. Res. 3 (2003) 1157–1182.

[27] M.V. Reddy, B.P. Muni, A. Sarma, Enhancement of voltage profile for IEEE 14 bus system with inter line power flow controller, in: 2016 Biennial International Conference on Power and Energy Systems: Towards Sustainable Energy, PESTSE, IEEE, 2016, pp. 1–5.

[28] B. Pal, B. Chaudhuri, Robust Control in Power Systems, Springer Science & Business Media, 2006.
[29] R. Henriquez-Auba, J.D. Lara, D.S. Callaway, C. Barrows, Transient simulations with a large penetration of converter-interfaced generation: Scientific computing challenges and opportunities, IEEE Electrif. Mag. 9 (2) (2021) 72–82, http://dx.doi.org/10.1109/MELE.2021.3070939.
[30] J.D. Lara, C. Barrows, D. Thom, D. Krishnamurthy, D. Callaway, PowerSystems. jl—A power system data management package for large scale modeling, SoftwareX 15 (2021) 100747.
[31] A.C. Hindmarsh, P.N. Brown, K.E. Grant, S.L. Lee, R. Serban, D.E. Shumaker, C.S. Woodward, Sundials: Suite of nonlinear and differential/algebraic equation solvers, ACM Trans. Math. Softw. 31 (3) (2005) 363–396.
[32] S. Bolognani, Grid topology identification via distributed statistical hypothesis testing, in: Big Data Application in Power Systems, Elsevier, 2018, pp. 281–301.
[33] J.L. Cremer, I. Konstantelos, G. Strbac, From optimization-based machine learning to interpretable security rules for operation, IEEE Trans. Power Syst. 34 (5) (2019) 3826–3836, http://dx.doi.org/10.1109/TPWRS.2019.2911598.
[34] H. Wang, Z. Lei, X. Zhang, B. Zhou, J. Peng, A review of deep learning for renewable energy forecasting, Energy Convers. Manage. 198 (2019) 111799.
[35] D.C. Park, M. El-Sharkawi, R. Marks, L. Atlas, M. Damborg, Electric load forecasting using an artificial neural network, IEEE Trans. Power Syst. 6 (2) (1991) 442–449.
[36] P. Pourbeik, J.J. Sanchez-Gasca, J. Senthil, J.D. Weber, P.S. Zadehkhost, Y. Kazachkov, S. Tacke, J. Wen, A. Ellis, Generic dynamic models for modeling wind power plants and other renewable technologies in large-scale power system studies, IEEE Trans. Energy Convers. 32 (3) (2017) 1108–1116, http://dx.doi.org/10.1109/TEC.2016.2639050.